

OPTIMIZATION OF ULTRASONIC PHASED ARRAYS

Shi-Chang Wooh and Yijun Shi

Department of Civil and Environmental Engineering
Massachusetts Institute of Technology
Cambridge, MA 02139

INTRODUCTION

Ultrasonic phased arrays are an emerging technology in nondestructive evaluation (NDE) applications. A phased array is a multi-element piezo-electric device whose elements are individually excited by electric pulses at programmed delay times [1]. Such a delay scheme allows electronically controlled dynamic beam control. One of the advantages of using phased arrays in NDE applications over conventional ultrasonic transducers is their great maneuverability of the ultrasonic beam, i.e., dynamic beam steering and focusing. This way, target materials can be rapidly inspected by electronically sweeping the sound beam in the area of interest without requiring mechanical or manual scanning.

Although phased arrays have been and are being used widely in the fields of medical diagnosis such as echocardiography and ultrasonography [2], their use in NDE is limited, due to a variety of reasons such as high cost of fabrication and complexity of wave motion in solid materials. For their effective use in NDE, the transducer should be designed optimally for testing materials.

In this paper, acoustic pressure distribution of the ultrasonic waves emitted from linear phased arrays was derived and the beam steering characteristics were studied. The influence of array element size is not discussed here but will appear elsewhere [3, 4]. The objective of the study is to investigate the influence of array parameters including inter-element spacing, wavelength and number of elements on the beam steerability and directivity for optimum beam steering efficiency.

THEORY—ACOUSTIC PRESSURE FIELD AND BEAM DIRECTIVITY

The linear phased array was modeled as a discrete number of simple sources separated by equal distances between the elements (d), as shown in Fig. 1. The pressure field was reconstructed using Huyghens' principle with properly selected phases and amplitudes, as follows

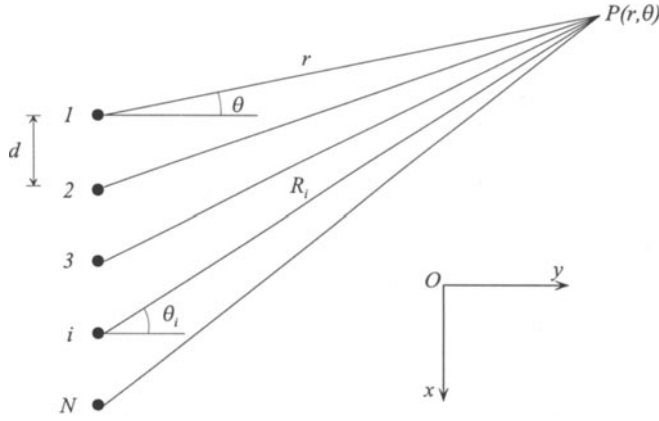


Figure 1. Acoustic waves radiated from an array of simple point sources.

$$p(r, \theta, t) = \frac{p_0 r_0}{r} \frac{\sin \left[\left(\frac{\omega \Delta \tau - kd \sin \theta}{2} \right) N \right]}{\sin \left(\frac{\omega \Delta \tau - kd \sin \theta}{2} \right)} \exp \left[-j \left(\frac{\omega \Delta \tau - kd \sin \theta}{2} \right) (N - 1) \right] \quad (1)$$

$$\times \exp [j(\omega t - kr)]$$

for $r \gg d$, where r_0 is the infinitesimally small radius of pulsating point sources, p_0 the pressure amplitude at the simple point sources, k the wave number, ω the angular frequency, N the number of point sources, and j is a unit imaginary number. The required time delay between the adjacent sources to steer the beam at an angle θ_s is given by the relationship [5]

$$\Delta \tau = \frac{d \sin \theta_s}{c} \quad (2)$$

where c is the wavespeed in the medium.

In order to understand the steering characteristics quantitatively, the *beam directivity* is analyzed here. The directivity, defined as the pressure at an angle normalized by the pressure at the steering angle, can be written from eq. (1) in the form

$$H(\theta) = \left| \frac{\sin \left[\frac{\pi d (\sin \theta_s - \sin \theta)}{\lambda} N \right]}{N \sin \left[\frac{\pi d (\sin \theta_s - \sin \theta)}{\lambda} \right]} \right|. \quad (3)$$

Phased arrays may be optimally designed by analyzing the directivity patterns and properly selecting transducer parameters that influence the wave propagation characteristics. Figure 2 is a schematic illustration that shows some important features of directivity plots. As shown in the figure, there are basically three kinds of directivity lobes: the main lobe, side lobes and grating lobes. The main lobe appears exactly in the steering direction (30° in this case), while *side lobes* appear in many directions other than the steering angle. In addition, there exists a third kind of lobe whose magnitude is exactly equal to the main lobe. These lobes are called *grating lobes*. The first grating lobe appears at the $(N - 1)$ th lobe location from the main lobe.

The steering performance can be characterized by the sharpness of the main lobe and the amount of side-leaking energy. Therefore, the goal of the optimum transducer design can be achieved by obtaining the condition for the sharpest main lobe while suppressing side lobes and squelching grating lobes.

Main Lobe Sharpness Factor

The beam directivity at an angle can be quantified by the width of the lobe in that direction that is defined by the distance between the zero-crossing points of the lobe. The main lobe sharpness is a quantitative representation of the beam directivity in the steering direction. This quantity is thus a very important parameter in designing a transducer. From eq. (3), the main lobe sharpness factor can be obtained as

$$q = \frac{1}{\pi} \left[\sin^{-1} \left(\sin \theta_s + \frac{\lambda}{Nd} \right) - \sin^{-1} \left(\sin \theta_s - \frac{\lambda}{Nd} \right) \right]. \quad (4)$$

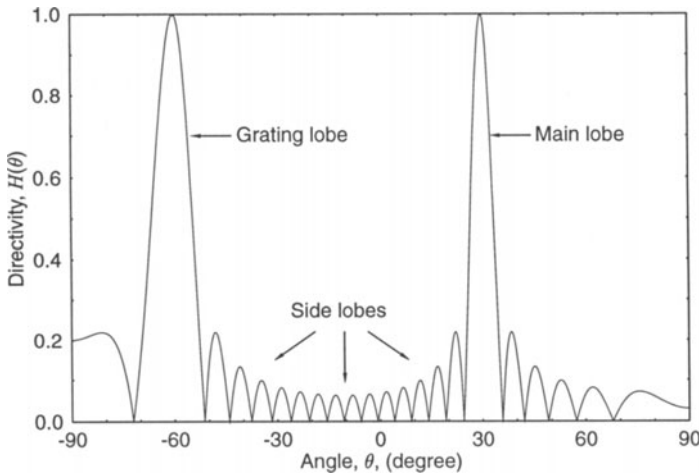


Figure 2. A typical directivity plot showing the main lobe, side lobes, and grating lobes.

Smaller q means that the lobe is sharp and the beam is finely directed. Note that if the term λ/Nd approaches zero, then q is compressed to zero. This means that the beam directivity can be improved by providing more elements or by increasing the distance between the elements. Also observe that q is a function of steering angle for a finite λ/dN . It is straightforward to show that q is an increasing function with θ_s for $0 \leq \theta_s \leq \pi/2$. Figure 3 shows the main lobe sharpness factor as a function of steering angle for a 16 element array whose inter-element spacing is half the wavelength. As expected, lobe sharpness increases and the directivity degrades with an increasing steering angle. The degradation rate is slow at first but accelerates very rapidly as the steering angle reaches certain value (in this case $\theta_s \approx 60^\circ$). We may conclude from this example that steering above 60° is not practical with this configuration.

Number of Elements N

One can observe from eq. (4) that q approaches zero for infinitely large number of elements ($N \rightarrow \infty$). This is an ideal condition but is impossible to achieve from a practical viewpoint mainly because of the limitations of control electronics. Furthermore, increasing number of elements also increases the transducer dimension. This may not be desirable since the transducer becomes bulkier and heavier due to extra backing and protective materials. Therefore, it is necessary to find a reasonably low number of elements that does not detrimentally affect these practical considerations.

Figure 4 shows the effect of N on the main lobe width. This plot was obtained for the steering angle of 30° . It is shown in the figure that the q -value sharply decreases for a very low number of elements ($N \leq 8$) and it decays asymptotically to zero with an increasing N . Improvement becomes marginal for the values of $N \geq 32$. Therefore, it can be argued that a 16 element array is sufficient to ensure reasonably good directivity for this particular case, which may be a reasonable compromise between transducer performance and cost.

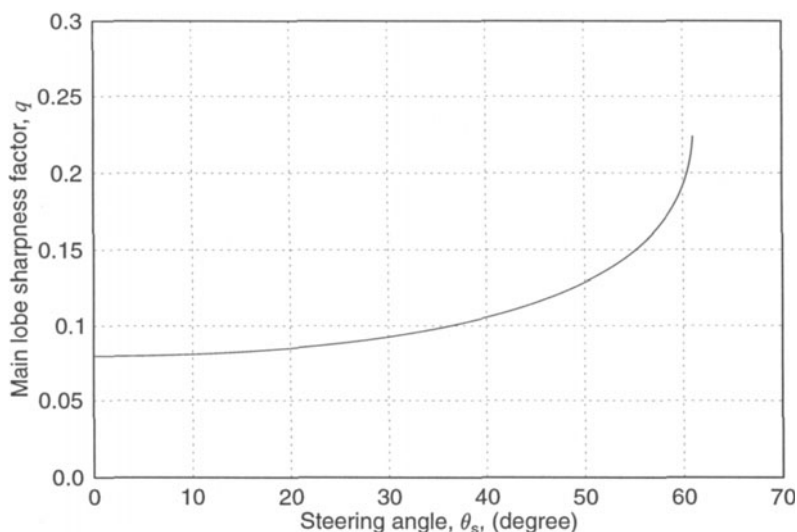


Figure 3. Main lobe sharpness factor as a function of steering angle ($N = 16$ and $d = \lambda/2$).

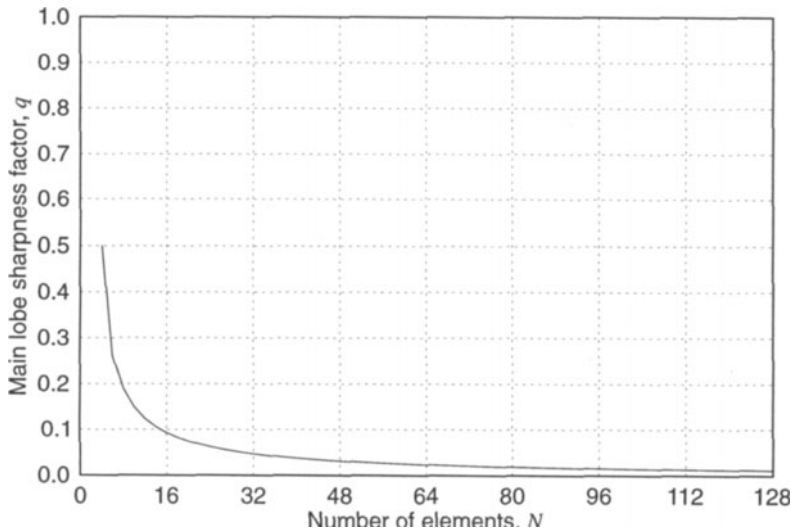


Figure 4. Main lobe sharpness factor as a function of number of elements ($d = \lambda/2$ and $\theta_s = 30^\circ$).

Inter-Element Spacing

The second way to reduce the main lobe sharpness factor is by providing a larger inter-element spacing for a fixed λ . In other words, beam directivity can be improved by increasing the spacing between the elements. Figure 5 presents the directivities in polar form, showing the effect of d on the beam directivity, again for $N = 16$ and $\theta_s = 0$. By comparing the lobe widths in Figs. 5(a), 5(b) and 5(c), one can observe that the beam directivity in the steering direction ($\theta_s = 30^\circ$) is greatly improved by increasing the inter-element spacing.

However, if the inter-element spacing d is too high, there are more side lobes and grating lobes produced. Figure 5(c) shows a directivity pattern for a large inter-element spacing ($d = 2\lambda$), whose directivity in the steering angle is better than the one shown in Fig. 5(b) ($d = \lambda/2$). At the same time, several grating lobes, whose magnitudes are equal to that of the main lobe, appear at the angles of 0° , -30° and $\pm 90^\circ$. The acoustic pressure field was numerically simulated. The simulation image confirming these trends in steel is shown in Fig. 6.

Critical Inter-Element Spacing

These grating lobes should be avoided since they result in spurious and confusing return signals. Therefore, we will find the critical inter-element spacing that introduces the first grating lobe, providing us with the best directivity, yet squelching grating lobes. This critical condition can be found from eq. (3) for $H(-\pi/2) = 1$, i.e., the inter-element spacing that satisfies the condition

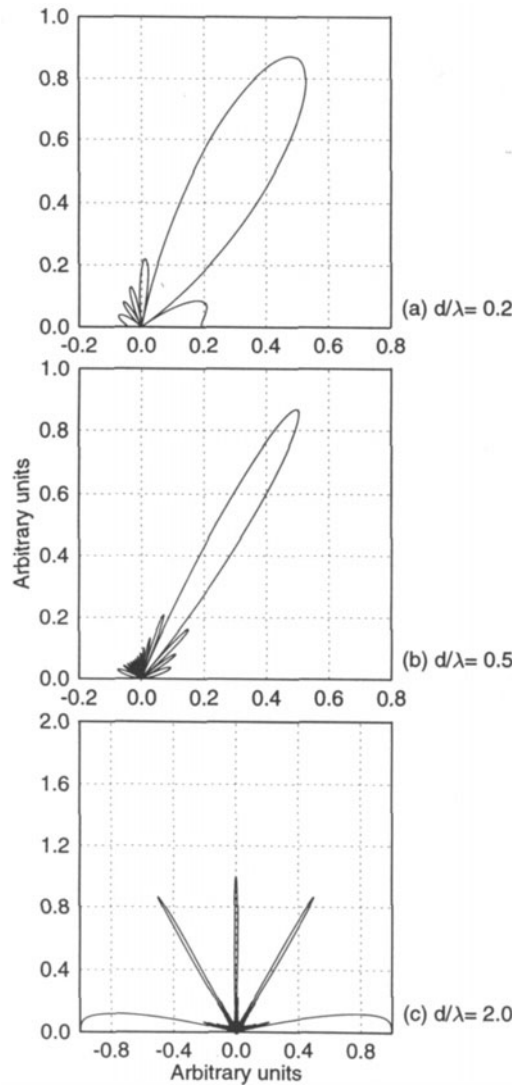


Figure 5. Effect of inter-element spacing on beam directivity characteristics ($\theta_s = 30^\circ$ and $N = 16$).

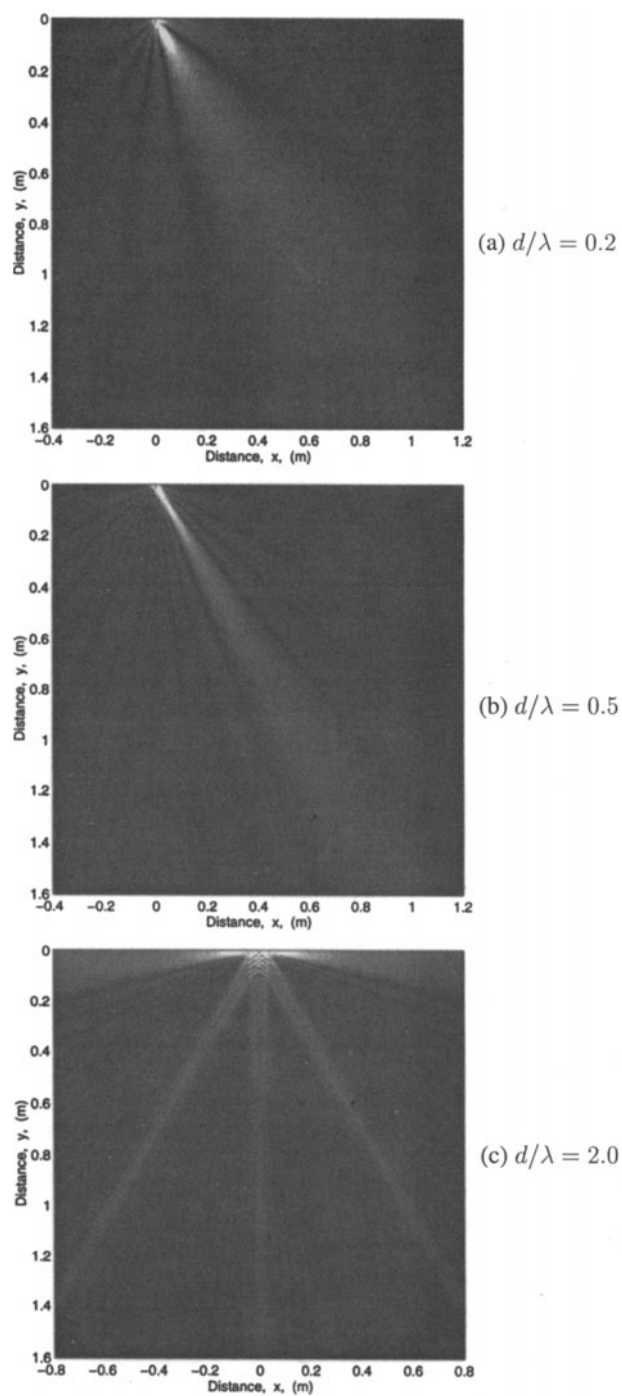


Figure 6. Simulated pressure fields of phased arrays in steel for various inter-element spacing ($\theta_s = 30^\circ$, $f = 2.3$ MHz, $N = 16$, $c = 5,850$ m/s).

$$\sin \theta = \sin \theta_s - \frac{\lambda}{d} \quad (5)$$

at $\theta = -90^\circ$ is the critical inter-element spacing d_{cr} . In other words,

$$d_{cr} = \frac{\lambda}{1 + \sin \theta_s} \quad (6)$$

where θ_s is the maximum desired steering angle.

SUMMARY AND CONCLUSIONS

The linear phased array was modeled as an ensemble of discrete point sources, excited by sequentially delayed pulses. The acoustic pressure field for the array was derived using Huyghens' principle and the corresponding directivity function was analyzed to find optimum inter-element spacing and number of elements. The transducer performance was quantified by the width of the main lobe that appears in the direction of the steering angle. The main lobe width was found by determining its zero-crossing points and quantified by the parameter q , main lobe sharpness factor. The design optimization was achieved by finding the conditions for the narrowest main lobe width.

It was found from this study that increasing number of elements improves the transducer performance. It is ideal to fabricate a transducer with infinitely large number of elements but there are physical limitations such as fabrication, bulkiness and complexity of control electronics. The approach discussed allows one to find a reasonably high number of elements that does not deteriorate the steering performance.

The beam steering characteristics can be also improved by selecting the inter-element spacing higher than the conventional limit of half the wavelength. However, the inter-element spacing should not be chosen too high, otherwise the deleterious grating lobes will appear. A critical inter-element spacing value was found in this study. In summary, the beam characteristics can be improved by limiting the maximum steering angle and increasing number of elements and inter-element spacing up to a limiting value.

ACKNOWLEDGMENTS

This work is supported by the Korea Highway Corporation. We are grateful to Dr. Chang-Guen Lee and Mr. Keon-Chang Cho for their encouragement and support.

REFERENCES

1. A. McNab and M. J. Campbell, "Ultrasonic phased arrays for nondestructive testing," *NDT Int.*, Vol. 6, 333–337, Dec. (1987).
2. A. E. Weyman, *Principles and Practice of Echocardiography*, (Lea & Febiger, Philadelphia), (1994).
3. S. C. Wooh and Y. Shi, *Optimum beam steering of linear phased arrays*, in preparation.
4. S. C. Wooh and Y. Shi, *Influence of the phased array element size on dynamic phase steering of ultrasound*, in preparation.
5. M. G. Silk, *Ultrasonic Transducers for Nondestructive Testing*, Adam Hilger Ltd, Bristol (1984).